Available online at www.sciencedirect.com
SCIENCE DIRECT®
Biochimica et Biophysica Acta 1758 (2006) 747–754
BIOCHIMICA ET BIOPHYSICA ACTA
BBA
http://www.elsevier.com/locate/bba

Substrate specificity of a chimera made from *Xenopus* SGLT1-like protein and rabbit SGLT1

Katsumi Nagata *, Yoshio Hata

Department of Biomedical Science, Institute of Regenerative Medicine and Biofunction, Tottori University Graduate School of Medical Science, Nishimachi 86, Yonago 683-8503, Japan

Received 28 December 2005; received in revised form 2 May 2006; accepted 4 May 2006
Available online 16 May 2006

Abstract

To characterize the sugar translocation pathway of Na^+/glucose cotransporter type 1 (SGLT1), a chimera was made by substituting the extracellular loop between transmembrane domain (TM) 12 and TM13 of *Xenopus* SGLT1-like protein (xSGLT1L) with the homologous region of rabbit SGLT1. The chimera was expressed in *Xenopus* oocytes and its transport activity was measured by the two-microelectrode voltage-clamp method. The substrate specificity of the chimera was different from those of xSGLT1L and SGLT1. In addition the chimera's apparent Michaelis–Menten constant (K_m) for *myo*-inositol, 0.06 mM, was about one fourth of that of xSGLT1L, 0.25 mM, while the chimera's apparent K_m for D-glucose, 0.8 mM, was about one eighth of that of xSGLT1L, 6.3 mM. Our results suggest that the extracellular loop between TM12 and TM13 participates in the sugar transport of SGLT1.
© 2006 Elsevier B.V. All rights reserved.

Keywords: *Xenopus* SGLT1-like protein; SGLT; SMIT; Chimera

1. Introduction

Na^+/glucose cotransporter type 1 (SGLT1) is one of the most intensively studied membrane transporters (reviews: [1,2]). SGLT1 is a member of the very large solute carrier family 5 (SLC5); this family has more than 220 members in procaryotes and eucaryotes (reviews: [3–5]). The proteins in this family transport various solutes (such as glucose, *myo*-inositol, amino acids and iodide) into cells using the Na^+ electrochemical potential gradient across the plasma membrane.

SGLT1 is present mainly in the intestine and kidney and takes up glucose and galactose into cells. It has been proposed that SGLT1 has 14 transmembrane domains (TMs) and displays the extracellular N- and C-termini [3,6]. Regarding the structure–function relationship, it is thought that the N-terminal half of SGLT1 participates in Na^+ transport [2,7–9] while the C-terminal half participates in sugar transport [2,10]. Ala-166 and Asp-454 are suggested to link the Na^+ and sugar translocation pathways [11,12]. However, except for a few residues responsible for sugar binding and/or translocation [2,13], the detailed structure of the sugar binding site of SGLT1 is yet unknown.

We have cloned and characterized an SGLT1 homologue from the *Xenopus laevis* intestine and named it *Xenopus* SGLT1-like protein (xSGLT1L) [14]. xSGLT1L transports *myo*-inositol better than D-glucose, and transports D-galactose and α-methyl-D-glucoside (αMG) (a specific substrate for SGLT) poorly, while SGLT1 transports D-glucose, D-galactose and αMG well, and transports *myo*-inositol poorly [15]. Therefore, the substrate specificity of xSGLT1L is similar to that of Na^+/*myo*-inositol cotransporter (SMIT) [15], another member of the SLC5 family, rather than that of SGLT1. Recently it was shown that xSGLT1L is a member of the ST1 subfamily in SLC5 [16]. According to its substrate specificity, ST1 has been renamed SMIT2 and the original or previously cloned SMIT has been renamed SMIT1 [17]. On the other hand, ST1 is called SGLT6 in the latest review [5]. Based on a comparison of the amino acid sequences among xSGLT1L, SGLT1 and SMIT1, we speculated that the extracellular loop between TM12 and TM13 must contain at least one crucial residue for sugar binding and/or translocation.

Making chimeras from SGLT1 and other members of the SLC5 family is one of the useful strategies for identifying residues

* Corresponding author. Tel.: +81 859 38 6252; fax: +81 859 38 6250.
E-mail address: knag@grape.med.tottori-u.ac.jp (K. Nagata).

0005-2736/$ - see front matter © 2006 Elsevier B.V. All rights reserved.
doi:10.1016/j.bbamem.2006.05.002

that participate in the sugar transport of SGLT1. The *xSGLT1L* cDNA has two useful restriction enzyme sites in TM12 and TM13 for making chimeras (see Fig. 1). In the present study, we made a chimera in which the extracellular loop between TM12 and TM13 of xSGLT1L was replaced by the homologous region of rabbit SGLT1, and examined its transport properties.

2. Materials and methods

2.1. Chimera generation

A chimeric protein was made by substituting the extracellular loop between TM12 and TM13 of xSGLT1L with the homologous region of rabbit SGLT1 (Fig. 1). The rabbit *SGLT1* cDNA was generously provided by Dr. E. M. Wright [18]. Using the rabbit *SGLT1* cDNA as template, a PCR fragment was obtained using the following primers: sense, 5′-GATTTTTCGAATGGTTCTCGATTTTATCTATG-GAACC-3′; and anti-sense, 5′-AAG*AAGCTT*ACAGCCACAACGACGAGGA-GAGTAAGGAGACCGAGGA-TCATGGACAAGTACAAGT-3′. The restriction site of *Csp* 45I is underlined and the site of *Hin*dIII is italicized. The positions of these two restriction sites in the *xSGLT1L* cDNA are shown in Fig. 1. There are no sites for these two enzymes in the corresponding region of the rabbit *SGLT1* cDNA. The primers were designed so that the PCR product encoded a polypeptide in which the amino acid sequence from Gly-507 to Gly-523 of rabbit SGLT1 (under the dotted line in Fig. 1) was conserved but the remainder of the sequence was replaced by that of xSGLT1L. After digestion by *Csp* 45I and *Hin*dIII, the PCR product was inserted into a plasmid containing the full-length *xSGLT1L* cDNA [14] that had been digested with the same enzymes. The nucleotide sequence of the chimeric cDNA was confirmed by sequencing.

cRNA was synthesized from the linearized plasmid containing the chimeric or *xSGLT1L* cDNA using an mCAP mRNA capping kit (Stratagene). The transcript was dissolved in diethyl pyrocarbonate (DEPC)-treated water at 0.5 μg/μl.

2.2. Expression and electrophysiology

A female frog (*Xenopus laevis*) was anesthetized in ice-cold water containing 0.1% ethyl *m*-aminobenzoate methanesulfonate. A piece of the ovary was surgically excised and incubated at 20 °C for 1 h in the presence of 1 mg/ml collagenase (type I, Sigma-Aldrich Co., St. Louis, MO) in Barth's solution. The composition of Barth's solution was 88 mM NaCl, 1 mM KCl, 2.4 mM $NaHCO_3$, 0.82 mM $MgSO_4$, 0.33 mM $Ca(NO_3)_2$, 0.91 mM $CaCl_2$, 10 mM HEPES–NaOH, pH 7.4, and 0.01 mg/ml penicillin and streptomycin. Then the oocytes in stages V–VI were defolliculated manually using tweezers. The defolliculated oocytes were incubated overnight at 20 °C in Barth's solution and viable oocytes were injected with 40–46 nl of cRNA solution with a glass micropipette using NANOJECT II (Drummond Scientific Co., Broomall, PA). The oocytes were incubated in Barth's solution at 20 °C, with daily medium changes until use.

Membrane currents from oocytes were measured by the two-microelectrode voltage-clamp method [14]. Briefly, the oocytes were superfused with a solution containing 88 mM NaCl, 2 mM KCl, 1.8 mM $CaCl_2$, and 10 mM HEPES–NaOH, pH 7.4. Oocytes were voltage clamped at −60 mV between 3 and 20 days after the injection. Measurements were done at room temperature (20–25 °C). Data acquisition and membrane voltage control were performed using pCLAMP 6 (Axon Instruments Inc., Union City, CA). Membrane currents were filtered at 100 Hz with an RC filter and sampled at 250 Hz, and records were further filtered at 10 Hz using pCLAMP 6.

2.3. Kinetic parameters

The chimera's apparent Michaelis–Menten constants (K_ms) for *myo*-inositol and D-glucose were calculated using OriginPro 7.5J (OriginLab Co., Northampton, MA).

The chimera's apparent inhibition constant (K_i) for phlorizin, which is a competitive inhibitor of xSGLT1L [14], as well as SGLT and SMIT, was calculated as follows (see Fig. 5). From one chimera-expressing oocyte currents induced by 1 and 20 mM *myo*-inositol in the presence of 0.1 mM phlorizin or 20 mM *myo*-inositol in the absence of phlorizin were recorded twice under each condition. The currents were plotted on an Eadie–Scatchard plot. In this plot the currents induced by 20 mM *myo*-inositol alone were plotted on the *x*-axis for two reasons: (1) this chimera exhibits the maximum current response (I_{max}) to 20 mM *myo*-inositol (see Discussion) and (2) I_{max} is the same whether phlorizin is present or not because inhibition by phlorizin is competitive. Then, the line was drawn by the least-squares method using OriginPro 7.5J. The line can be described by the equation

$$I_m/[MI] = -I_m/K_m' + I_{max}/K_m' \quad (1)$$

where I_m is the current elicited by the chimera, [MI] is the concentration of *myo*-inositol and K_m' is the apparent Michaelis–Menten constant in the presence of inhibitor. Finally the apparent K_i was calculated using the following equation [19]:

$$K_m' = K_m(1 + [I]/K_i) \quad (2)$$

where K_m is the apparent Michaelis–Menten constant in the absence of inhibitor and [I] is the concentration of inhibitor.

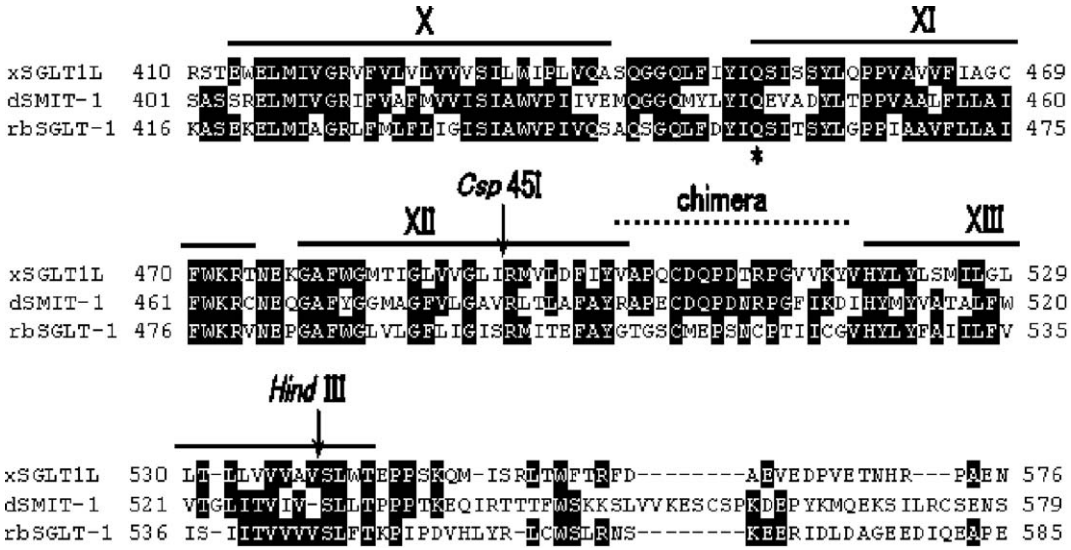

Fig. 1. Amino acid sequence alignment of *Xenopus* SGLT1-like protein (xSGLT1L), dog SMIT1 (dSMIT-1) and rabbit SGLT1 (rbSGLT-1). Part of the complete coding sequence is shown. Amino acids conserved in two or three of the proteins are shaded black. Bars labeled with Roman numerals indicate putative TMs. The dotted line labeled 'chimera' indicates the region used to make the chimera. Arrows indicate the positions of two restriction sites, *Csp* 45I and *Hin*dIII, in the *xSGLT1L* cDNA. The asterisk denotes Gln-457 in rabbit SGLT1. Sequence alignment was performed using GENETYX-SV/RC version 6 (Software Development, Tokyo, Japan).

3. Results

3.1. Sequence comparison of xSGLT1L, SMIT1 and SGLT1

Fig. 1 shows a part of the sequence alignment of xSGLT1L [14], dog SMIT1 [20] and rabbit SGLT1 [18]. Putative TMs are assigned according to the 14 membrane-spanning model of SGLT1 [3,6]. It is thought that the sugar permeation pathway of SGLT1 utilizes TM10–13 because a truncated SGLT1 which was made from the last 5 TMs (TM10–14) worked as a glucose uniporter [10] and some members of the SLC5 family lack the 14th TM [3,4]. The overall amino acid sequence of xSGLT1L shares 53% identity with that of rabbit SGLT1 and 46% identity with that of dog SMIT1. Therefore, the extracellular loop between TM12 and TM13 is somewhat anomalous, because the loop of xSGLT1L is very similar to that of dog SMIT1 but is not so similar to that of rabbit SGLT1. We hypothesized that important amino acids in sugar binding and/or translocation are located in this loop, and made a chimeric protein in which the extracellular loop between TM12 and TM13 (including the last amino acid of TM12) of xSGLT1L was replaced by the homologous region of rabbit SGLT1.

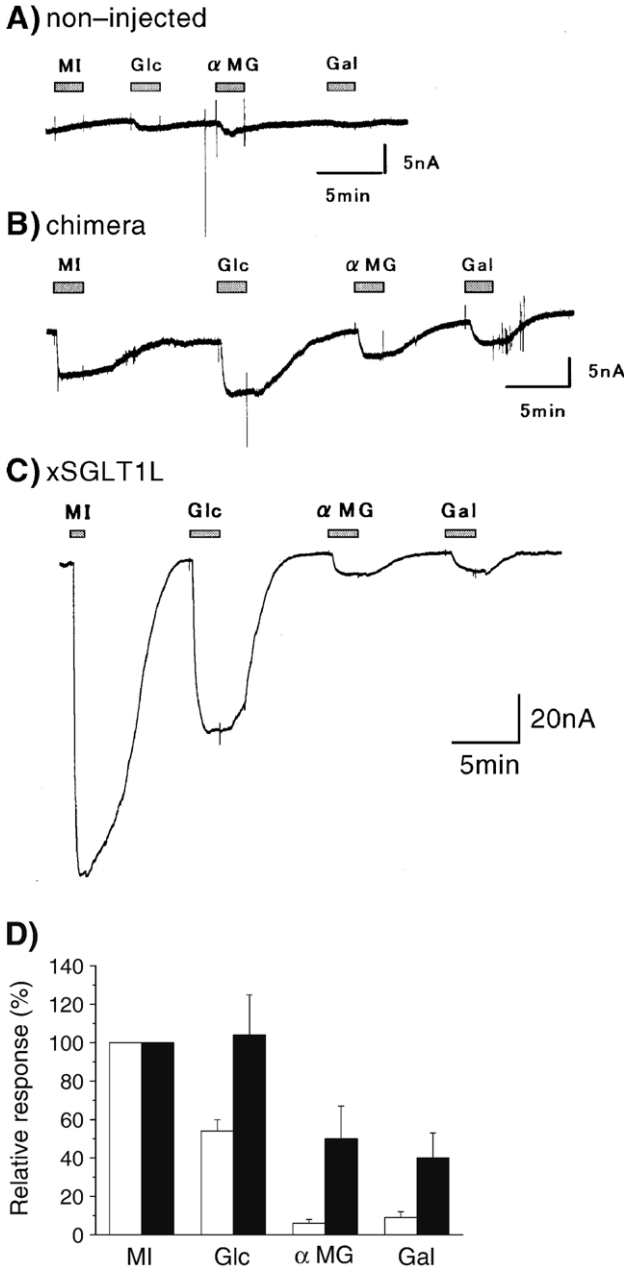

Fig. 2. Substrate specificity of the chimera and xSGLT1L. Membrane current recordings are shown. (A) Non-injected (control), (B) chimeric cRNA-injected and (C) *xSGLT1L* cRNA-injected oocyte. Inward currents are shown in the downward direction. Oocytes were clamped at −60 mV and superfused with substrates: MI, *myo*-inositol; Glc, D-glucose; αMG, α-methyl-D-glucoside; Gal, D-galactose. Substrate concentrations were all 20 mM. Superfusion periods are indicated by shaded boxes above the traces. Oocytes in A–C were from the same batch; B and C were recorded 12 days after the injection and A was recorded 14 days after the defolliculation. (D) relative amplitude of the substrate-induced current in chimera- or xSGLT1L-expressing oocytes. Open boxes, xSGLT1L, $n=6$; closed boxes, chimera, $n=14$: error bars denote SD.

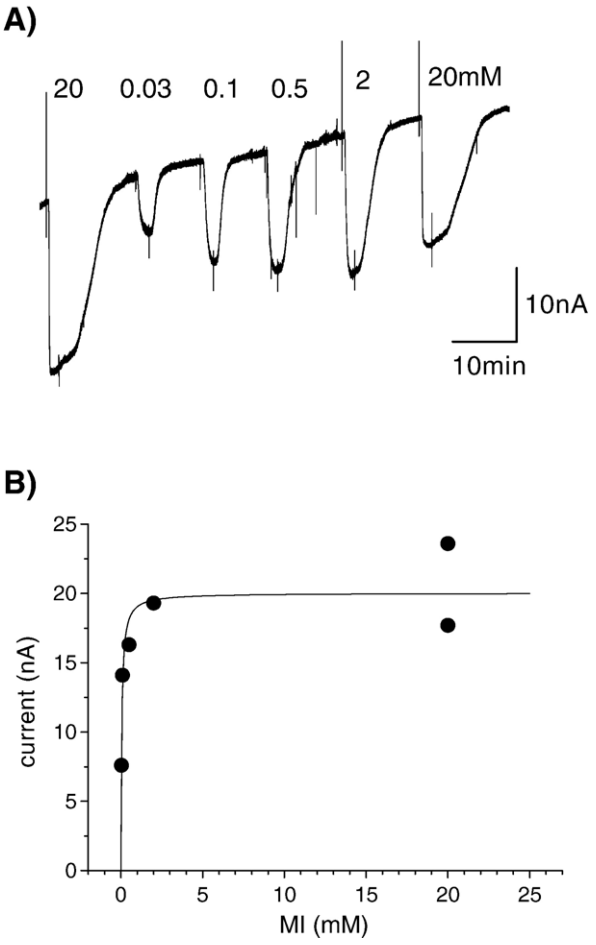

Fig. 3. *myo*-inositol dependency of the chimera. (A) A current record from a chimera-expressing oocyte is shown. The downward direction means the inward current. Concentrations of *myo*-inositol are indicated above the current trace. This oocyte was voltage clamped at −60 mV 12 days after the injection. (B) Current responses in A were plotted against *myo*-inositol concentration. The solid line was curve fitted by Michaelis–Menten-type kinetics with $I_{max}=20.0$ nA and the apparent $K_m=0.05$ mM.

3.2. Expression of the chimera

In control oocytes, 20 mM D-glucose and αMG induced small inward currents (Fig. 2A) that were probably due to the

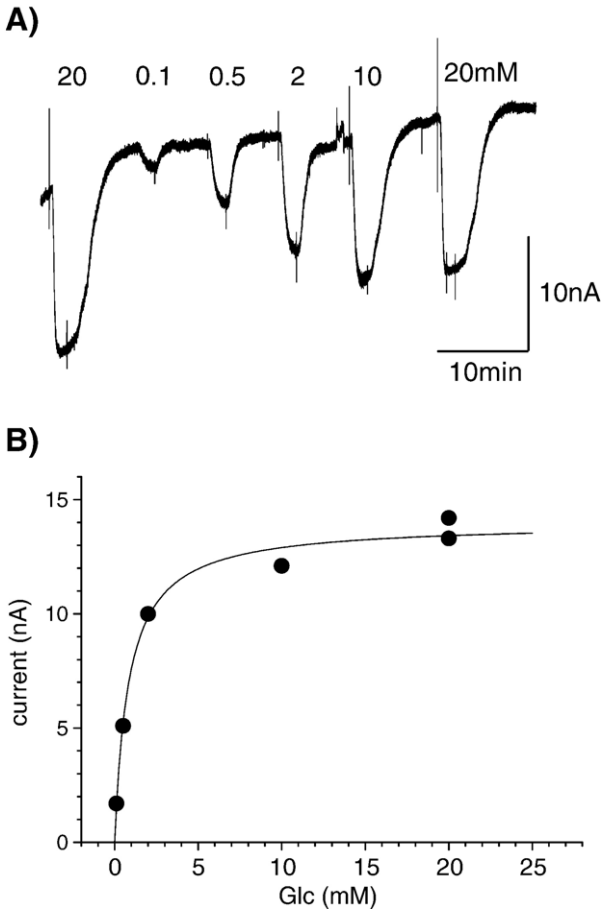

Fig. 4. D-glucose dependency of the chimera. (A) A current record from a chimera-expressing oocyte is shown. Concentrations of D-glucose are indicated above the current trace. This oocyte was voltage clamped at −60 mV 15 days after the injection. (B) Current responses in A were plotted against D-glucose concentration. The solid line was curve fitted by Michaelis–Menten-type kinetics with I_{max}=14.0 nA and the apparent K_m=0.8 mM.

endogenous SGLT in *Xenopus* oocytes [14,21–23]. In our experience the endogenous current was not always observed and never exceeded 2 nA.

Fig. 2B shows the transport current elicited by the chimera expressed in *Xenopus* oocytes. Expression of the chimera was much weaker than that of xSGLT1L (Fig. 2C). In the batch of oocytes (all obtained at one time from one frog) shown in Fig. 2A–C, the 20 mM *myo*-inositol-induced current of the chimera was 6.5±1.7 nA (mean±SD, n=6) while that of xSGLT1L was 71±48 nA (n=4), when the membrane potential was held at −60 mV. Using four batches of oocytes, we compared the expression between the chimera and xSGLT1L. The relative amplitude of the 20 mM *myo*-inositol-induced current of the chimera was 17±6% (n=4) when normalized by that of xSGLT1L in each batch. The transport current of the chimera never exceeded 30 nA.

The substrate specificity of the chimera is compared with that of xSGLT1L in Fig. 2D. The peak amplitude of substrate-induced current in each chimera- or xSGLT1L-expressing oocyte was normalized relative to the *myo*-inositol-induced current in each oocyte. Substrate concentrations were all 20 mM. The data for the chimera were obtained from two batches: data from one batch are shown in Fig. 2A–C and in the other batch the 20 mM *myo*-inositol-induced current was 11.0±3.8 nA (mean±SD, n=8). Data on xSGLT1L in Fig. 2D are from our previous report [14]. The substrate specificity of the chimera was different from those of xSGLT1L and SGLT1. The order of substrate specificity of SGLT1 was αMG ≈D-glucose ≈D-galactose ≫*myo*-inositol [15].

It should be noted that the chimera's relative responses elicited by D-glucose and αMG might have been overestimated due to the endogenous SGLT activity in *Xenopus* oocytes. Also the extent of overestimation for αMG would be larger than that for D-glucose because the chimera's current induced by D-glucose was about two times larger than that induced by αMG whereas the endogenous currents induced by the two sugars are almost the same. The overestimation was at most 20% for αMG (data not shown).

Fig. 3 shows the *myo*-inositol dependence of the chimera recorded from one oocyte. The current amplitude obeyed Michaelis–Menten-type kinetics with *myo*-inositol concentration, and in this example the apparent K_m was 0.05 mM (Fig. 3B, the solid line). From six oocytes in two batches the chimera's apparent K_m for *myo*-inositol was 0.06±0.02 mM and I_{max} was 11.0±6.4 nA at the membrane potential of −60 mV. The chimera's apparent K_m for *myo*-inositol was about one fourth of that of xSGLT1L, 0.25±0.07 mM (n=7) [14].

Fig. 4 shows the D-glucose dependence of the chimera recorded from one oocyte. The current amplitude obeyed Michaelis–Menten-type kinetics with D-glucose concentration, and in this example, the apparent K_m was 0.8 mM (Fig. 4B, the solid line). From five oocytes in two batches the chimera's apparent K_m for D-glucose was 0.8±0.2 mM and I_{max} was 7.7±4.3 nA at the membrane potential of −60 mV. Because the control or endogenous current elicited by 20 mM D-glucose was only 0.3±0.3 nA (n=6) in the two batches, we ignored it in calculating kinetic parameters. The chimera's apparent K_m for D-glucose was about one eighth of that of xSGLT1L, 6.3±1.2 mM (n=5)[14].

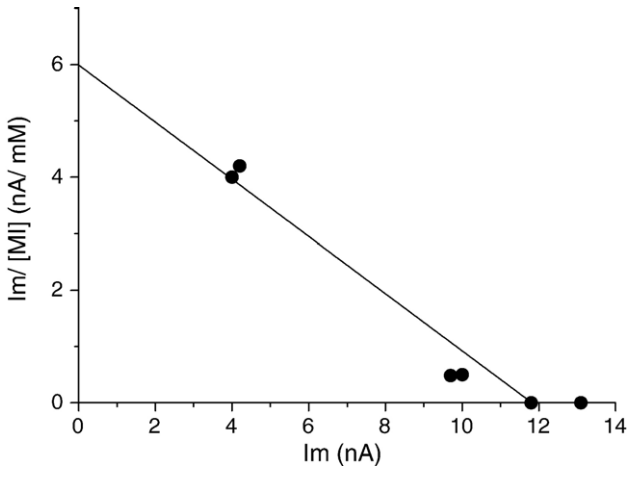

Fig. 5. Inhibition of the chimera by phlorizin. Currents induced by 1 and 20 mM *myo*-inositol in the presence of 0.1 mM phlorizin or 20 mM *myo*-inositol in the absence of phlorizin from one chimera-expressing oocyte were plotted on an Eadie–Scatchard plot. The line was drawn by the least-squares method. In this example, the apparent K_i for phlorizin was 3.1 μM. This oocyte was voltage clamped at −60 mV 19 days after the injection.

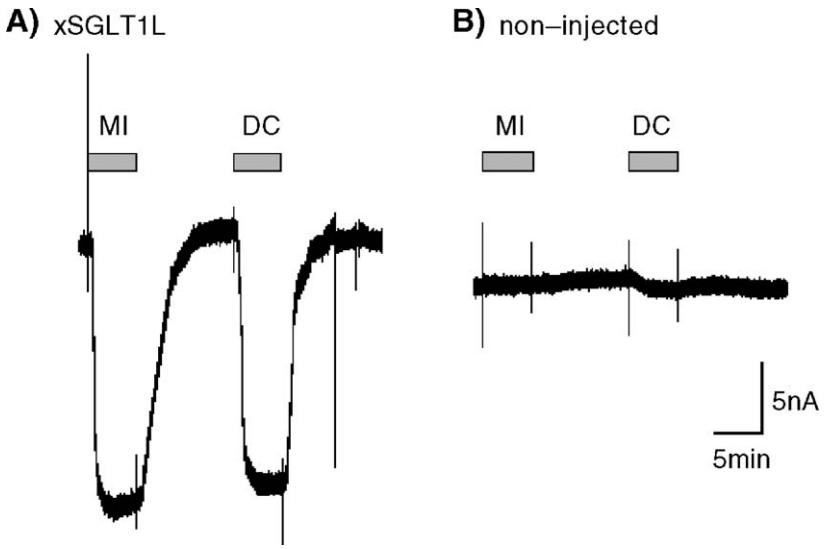

Fig. 6. D-*chiro*-inositol (DC) response of xSGLT1L. Membrane current recordings are shown. (A) *xSGLT1L* cRNA-injected and (B) non-injected (control) oocyte. Concentrations of DC and MI were 1 mM. The membrane potential was held at −60 mV. Oocytes in A and B were from the same batch; A was recorded 6 days after the injection and B was recorded 7 days after the defolliculation.

The chimera's apparent inhibition constant (K_i) for phlorizin, a competitive inhibitor of xSGLT1L, SGLT and SMIT, was calculated as shown in Fig. 5 (see Materials and methods). From four oocytes in two batches the apparent K_i for phlorizin was 3.6± 1.0 μM and I_{max} was 7.3±3.5 nA at the membrane potential of −60 mV. On the other hand, the apparent K_i of xSGLT1L for phlorizin was 7.3±2.3 μM (n=7) [14]. We are unable to discern a significant difference between the K_i values for phlorizin differ between xSGLT1L and the chimera.

3.3. D-chiro-inositol response of xSGLT1L

xSGLT1L is most closely related to rabbit SMIT2 [24]: they are 67% identical in amino acid sequence. However, whether xSGLT1L and SMIT2 are orthologous or not has been ambiguous [17]. SMIT2 transports D-*chiro*-inositol as well as *myo*-inositol [17], so we examined the D-*chiro*-inositol response in xSGLT1L-expressing oocytes. When superfused with 1 mM D-*chiro*-inositol, xSGLT1L induced a current comparable to that induced by 1 mM *myo*-inositol (Fig. 6A). The same results were obtained in eight additional xSGLT1L-expressing oocytes from three batches. Our results suggest that xSGLT1L and SMIT2 are orthologous.

4. Discussion

The structure–function relationship of SGLT1 is largely unknown because of the lack of crystallographic data. However, a general outline has emerged: the Na^+ translocation pathway consists of the N-terminal half [2,7–9] and the sugar translocation pathway consists of the residual C-terminal half [2,10]. Furthermore, it has been reported that in SGLT1, Gln-457 is important for sugar binding and translocation [13] and Thr-460 participates in discrimination between D-glucose and D-galactose [13,17]. To search for amino acids other than Gln-457 and Thr-460 that are important for sugar transport, we compared the amino acid sequence from TM10 to TM13 among xSGLT1L, dog SMIT1 and rabbit SGLT1 (Fig. 1). We speculated that the extracellular loop between TM12 and TM13 must be important for sugar transport because in this loop the amino acid sequence of xSGLT1L is similar to that of dog SMIT1 but not to that of rabbit SGLT1, while with respect to substrate specificity, xSGLT1L is similar to SMIT1 rather than SGLT1 [14,15].

4.1. Weak expression of the chimera

We made a chimeric protein in which the extracellular loop between TM12 and TM 13 of xSGLT1L (including the last amino acid of TM12) was replaced by the homologous region of rabbit SGLT1 (Fig. 1), and expressed it in *Xenopus* oocytes. Before performing the experiments, we expected that the chimera would be expressed well because both xSGLT1L and SGLT1 are expressed well in *Xenopus* oocytes [1,13–15]. However, the current elicited by the chimera was about one sixth of that elicited by xSGLT1L and never exceeded 30 nA (see Results).

We think that the weak expression of the chimera was probably due to a defect in targeting of the protein to the plasma membrane. It has been reported that 22 out of the 23 missense mutations identified in glucose–galactose malabsorption (GGM) did not reach the plasma membrane when expressed in *Xenopus* oocytes [25]. In our chimera the substitutions observed in GGM did not occur, but some of the substituted amino acids in our chimera might have affected the targeting. In addition, it was shown that the surface density of the chimera named C1, in which the N-terminal 69 amino acids of SGLT1 were replaced by the first 50 amino acids of SMIT1, was about one seventh that of SGLT1 in the *Xenopus* oocyte plasma membrane [26]. This means that the substitution of the homologous region even between SGLT1 and SMIT1 might decrease the stability of C1 and/or induce incorrect targeting of C1. The same kind of disturbance might have affected our chimera.

4.2. Substrate specificity of the chimera

Before considering the substrate specificity of the chimera, we note that whether xSGLT1L and SMIT2 are orthologous or not has been ambiguous [17]. The most obvious difference between the two proteins is their tissue distribution: for example, xSGLT1L is expressed in the intestine [14] but SMIT2 is not [24,27]. In the present study we showed that xSGLT1L transported D-*chiro*-inositol as well as *myo*-inositol (Fig. 6). SMIT2 also transports both substances to the same extent [17], and therefore we think the two proteins are orthologous. As pointed out by Coady et al. [17], in the course of evolution the two proteins have acquired somewhat different roles between amphibians and mammals.

The substrate specificity of the chimera was different from those of xSGLT1L (Fig. 2) and SGLT1 [15]. Two obvious features of the substrate specificity of the chimera are as follows: (1) the currents induced by 20 mM *myo*-inositol and D-glucose were almost the same in amplitude and (2) the relative responses elicited by 20 mM αMG and D-galactose were larger than those of xSGLT1L.

We think that the chimera's apparent affinities for the four substrates we tested increased simultaneously. Also the first feature of the chimera's substrate specificity can be explained by the fact that the chimera's apparent K_ms for *myo*-inositol and D-glucose are 0.06 and 0.8 mM while those of xSGLT1L are 0.25 mM and 6.3 mM [14]. In the Michaelis–Menten-type kinetics (where *myo*-inositol and D-glucose show the same I_{max}), the 20 mM D-glucose-induced current increases from 76 to 96% of I_{max} when the apparent K_m decreases from 6.3 to 0.8 mM, whereas the 20 mM *myo*-inositol-induced current increases from 99 to 100% of I_{max} when the apparent K_m decreases from 0.25 to 0.06 mM [19]. Although 76% of I_{max}, the theoretical xSGLT1L response induced by 20 mM D-glucose, is somewhat larger than the measured value, 54±6% (Fig. 2D), our explanation would still be essentially correct.

It has been thought that the amino acid at position 460 is important in the discrimination between D-glucose and D-galactose [13,17]. SGLT1 has Thr-460 and transports D-glucose and D-galactose equally [15] whereas SGLT2 and SMIT2 (including xSGLT1L) have Ser at that position (Ser-460) and prefer D-glucose to D-galactose as a substrate [14,17,30,33].The fact that the chimera contained Ser-460 and had a higher affinity for D-glucose as compared to D-galactose supports the notion that Ser-460 plays a critical role in the substrate recognition of SGLT.

We compare the region used to make the chimera among SMIT2 (including xSGLT1L), SMIT1, SGLT1 and SGLT2 in Fig. 7. In this figure, amino acids conserved in three or five orthologues are shown. This figure shows that the sequences are fairly different between SMIT and SGLT, and seven amino acids are different between SMIT2 and SGLT1 (and conserved in each orthologue): (numbers in SGLT1) Gly-507, Gly-509, Glu-513, Ser-515, Cys-517, Ile-521 and Cys-522. Of these seven amino acids Glu-513 (the arrow in Fig. 7) is most interesting. Human SGLT2 has Gln [28] as well as in SMIT1 and SMIT2, whereas mouse, rat, rabbit and bovine SMIT2 have Arg [29–32] at that position. The apparent K_m for αMG is 3.0 mM in rat SGLT2 (Arg-513, +1 charge) [30], and this value is about two times larger than that of human SGLT2 (Gln-513, 0), 1.6 mM [33]. The affinity is further increased in SGLT1 (Glu-513, −1); the apparent K_m for αMG is 0.05–0.5 mM in rat, human and rabbit SGLT1 [34]. Therefore, Glu-513 or its −1 charge may be important for the high affinity of SGLT1 for D-glucose and αMG. We also speculate that the increase in the apparent affinity for D-glucose of the chimera was at least partly due to the Gln-513-Glu substitution.

Lately it has been reported that Cys-255 and Cys-511 (the arrowhead in Fig. 7) make a disulfide bond in SGLT1 [41]. By breaking this disulfide bond the Q–V curve of the presteady-state current was shifted by +25 mV and the apparent K_m for αMG was increased by 60%. Although the authors of that study did not explain why the apparent K_m was increased, we think that a small change in the loop structure induced by breaking the disulfide bond might be the cause.

Our results clearly show that the extracellular loop between TM12 and TM13 participates in the sugar transport of SGLT1. Although the loop may not be a part of the sugar binding site, but it may work as a kind of a selectivity filter at the entrance of the sugar translocation pathway.

4.3. Phlorizin binding

The chimera's apparent K_i for phlorizin was not different from that of xSGLT1L (see Results). This is probably because the apparent K_i is mainly determined by the interaction between the protein and the aglucone of phlorizin. However, which region of SGLT1 interacts with the aglucone of phlorizin cannot be inferred from our results on the chimera.

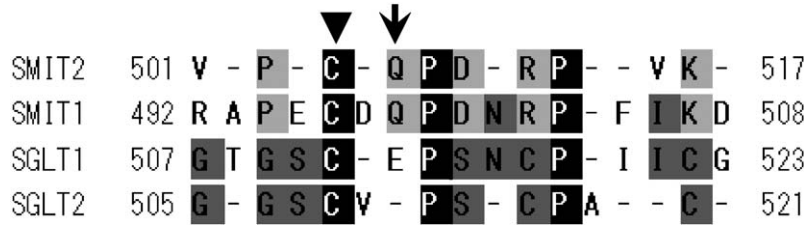

Fig. 7. Sequence comparison of the region used to make the chimera. SMIT2 includes xSGLT1L. Hyphens indicate amino acids that differ in orthologues. Amino acids conserved in four proteins are shaded black, and those conserved in two proteins are shaded dark or light gray. The arrowhead and arrow indicate the positions of Cys-511 and Glu-513, respectively, in SGLT1. Orthologues included in the figure are as follows: xSGLT1L [14] and human [27] and rabbit SMIT2 [24]; human, dog and bovine SMIT1 [40]; human, mouse, rat, rabbit and pig SGLT1 [3]; human, mouse, rat, rabbit and bovine SGLT2 [32].

Recently it has been proposed that the amino acids from 604 to 610 (aa 604–610) of SGLT1 bind to the aglucone of phlorizin [35,36]. The authors of those studies claimed that the region aa 604–610 is extracellular [37]. However, according to the 14 membrane-spanning model of the SLC5 family, this region is intracellular [2–4,6,38]. Lately it was also suggested that the large loop between TM13 and TM14, namely aa 549–639, of SGLT1 would start and finish at an intracellular localization and could form some kind of re-entrant loop, allowing accessibility from the extracellular solution [39]. This re-entrant loop model seems to be compatible with most of the results concerning the position of the loop; however, the authors of this model also suggest that the loop does not appear to play a major part in the binding of phlorizin [39].

Acknowledgement

We are grateful to Dr. E. M. Wright (Department of Physiology, David Geffen School of Medicine at UCLA, Los Angeles, CA, USA) for providing the rabbit *SGLT1* cDNA.

References

[1] M.A. Hediger, D.B. Rhoads, Molecular physiology of sodium-glucose cotransporters, Physiol. Rev. 74 (1994) 993–1026.
[2] E.M. Wright, Renal Na^+-glucose cotransporters, Am. J. Physiol., Renal Fluid Electrolyte Physiol. 280 (2001) F10–F18.
[3] E. Turk, E.M. Wright, Membrane topology motifs in the SGLT cotransporter family, J. Membr. Biol. 159 (1997) 1–20.
[4] H. Jung, The sodium/substrate symporter family: structural and functional features, FEBS Lett. 529 (2002) 73–77.
[5] E.M. Wright, E. Turk, The sodium/glucose cotransport family SLC5, Pflügers Arch. 447 (2004) 510–518.
[6] E. Turk, C.J. Kerner, M.P. Lostao, E.M. Wright, Membrane topology of the human Na^+/glucose cotransporter SGLT1, J. Biol. Chem. 271 (1996) 1925–1934.
[7] B. Lo, M. Silverman, Cysteine scanning mutagenesis of the segment between putative transmembrane helices IV and V of the high affinity Na^+/glucose cotransporter SGLT1, J. Biol. Chem. 273 (1998) 29341–29351.
[8] M. Quick, D.D.F. Loo, E.M. Wright, Neutralization of a conserved amino acid residue in the human Na+/glucose transporter (hSGLT1) generates a glucose-gated H^+ channel, J. Biol. Chem. 276 (2001) 1728–1734.
[9] S.A. Huntley, D. Krofchick, M. Silverman, Position 170 of rabbit Na^+/glucose cotransporter (rSGLT1) lies in the Na^+ pathway; modulation of polarity/charge at this site regulates charge transfer and carrier turnover, Biophys. J. 87 (2004) 295–310.
[10] M. Panayotova-Heiermann, S. Eskandari, E. Turk, G.A. Zampighi, E.M. Wright, Five transmembrane helices form the sugar pathway through the Na+/glucose cotransporter, J. Biol. Chem. 272 (1997) 20324–20327.
[11] A.-K. Meinild, D.D.F. Loo, B.A. Hirayama, E. Gallardo, E.M. Wright, Evidence for the involvement of Ala 166 in coupling Na^+ to sugar transport through the human Na^+/glucose cotransporter, Biochemistry 40 (2001) 11897–11904.
[12] A. Díez-Sampedro, D.D.F. Loo, E.M. Wright, G.A. Zampighi, B.A. Hirayama, Coupled sodium/glucose cotransport by SGLT1 requires a negative charge at position 454, Biochemistry 43 (2004) 13175–13184.
[13] A. Díez-Sampedro, E.M. Wright, B.A. Hirayama, Residue 457 controls sugar binding and transport in the Na^+/glucose cotransporter, J. Biol. Chem. 276 (2001) 49188–49194.
[14] K. Nagata, N. Hori, K. Sato, K. Ohta, H. Tanaka, Y. Hiji, Cloning and functional expression of an SGLT-1-like protein from the *Xenopus laevis* intestine, Am. J. Physiol. 276 (1999) G1251–G1259.
[15] K. Hager, A. Hazama, H.M. Kwon, D.D.F. Loo, J.S. Handler, E.M. Wright, Kinetics and specificity of the renal Na^+/myo-inositol cotransporter expressed in *Xenopus* oocytes, J. Membr. Biol. 143 (1995) 103–113.
[16] S.R. Eid, A. Terrettaz, K. Nagata, A.W. Brändli, Embryonic expression of *Xenopus* SGLT-1L, a novel member of the solute carrier family 5 (SLC5), is confined to tubules of the pronephric kidney, Int. J. Dev. Biol. 46 (2002) 177–184.
[17] M.J. Coady, B. Wallendorff, D.G. Gagnon, J.-Y. Lapointe, Identification of a novel Na^+/*myo*-inositol cotransporter, J. Biol. Chem. 277 (2002) 35219–35224.
[18] M.A. Hediger, M.J. Coady, T.S. Ikeda, E.M. Wright, Expression cloning and cDNA sequencing of the Na^+/glucose co-transporter, Nature 330 (1987) 379–381.
[19] J.M. Berg, J.L. Tymoczko, L. Stryer, Biochemistry, Fifth edition, W.H. Freeman and Company, New York, 2002, pp. 200–210.
[20] H.M. Kwon, A. Yamauchi, S. Uchida, A.S. Preston, A. Garcia-Perez, M.B. Burg, J.S. Handler, Cloning of the cDNA for a Na^+/*myo*-inositol cotransporter, a hypertonicity stress protein, J. Biol. Chem. 267 (1992) 6297–6301.
[21] W.-M. Weber, W. Schwarz, H. Passow, Endogenous D-glucose transport in oocytes of *Xenopus laevis*, J. Membr. Biol. 111 (1989) 93–102.
[22] K. Nagata, O. Ichikawa, Two endogenous methyl-α-D-glucopyranoside uptake activities in *Xenopus* oocytes, Comp. Biochem. Physiol. 112B (1995) 115–122.
[23] T. Blasco, J.J. Aramayona, A.I. Alcalde, J. Catalán, M. Sarasa, V. Sorribas, Rat kidney MAP17 induces cotransport of Na/mannose and Na/glucose in *Xenopus laevis* oocytes, Am. J. Physiol., Renal Fluid Electrolyte Physiol. 285 (2003) F799–F810.
[24] K. Hitomi, N. Tsukagoshi, cDNA sequence for rkST1, a novel member of the sodium ion-dependent glucose cotransporter family, Biochim. Biophys. Acta 1190 (1994) 469–472.
[25] E.M. Wright, E. Turk, M.G. Martin, Molecular basis for glucose–galactose malabsorption, Cell Biochem. Biophys. 36 (2002) 115–121.
[26] M.J. Coady, F. Jalal, P. Bissonnette, M. Cartier, B. Wallendorff, G. Lemay, J.-Y. Lapointe, Functional studies of a chimeric protein containing portions of the Na^+/glucose and Na^+/*myo*-inositol cotransporters, Biochim. Biophys. Acta 1466 (2000) 139–150.
[27] P. Roll, A. Massacrier, S. Pereira, A. Robaglia-Schlupp, P. Cau, P. Szepetowski, New human sodium/glucose cotransporter gene (KST1): identification, characterization, and mutation analysis in ICAA (infantile convulsions and choreoathetosis) and BFIC (benign familial infantile convulsions) families, Gene 285 (2002) 141–148.
[28] R.G. Wells, A.M. Pajor, Y. Kanai, E. Turk, E.M. Wright, M.A. Hediger, Cloning of a human kidney cDNA with similarity to the sodium–glucose cotransporter, Am. J. Physiol. 263 (1992) F459–F465.
[29] N.M. Tabatabai, S.S. Blumenthal, D.L. Lewand, D.H. Petering, Differential regulation of mouse kidney sodium-dependent transporters mRNA by cadmium, Toxicol. Appl. Pharmacol. 177 (2001) 163–173.
[30] G. You, W.-S. Lee, E.J.G. Barros, Y. Kanai, T.-L. Huo, S. Khawaja, R.G. Wells, S.K. Nigam, M.A. Hediger, Molecular characteristics of Na^+-coupled glucose transporters in adult and embryonic rat kidney, J. Biol. Chem. 270 (1995) 29365–29371.
[31] A.M. Pajor, E.M. Wright, Cloning and functional expression of a mammalian Na+/nucleoside cotransporter, J. Biol. Chem. 267 (1992) 3557–3560.
[32] F.-Q. Zhao, T.B. McFadden, E.H. Wall, B. Dong, Y.-C. Zheng, Cloning and expression of bovine sodium/glucose cotransporter SGLT2, J. Dairy Sci. 88 (2005) 2738–2748.
[33] Y. Kanai, W.-S. Lee, G. You, D. Brown, M.A. Hediger, The human kidney low affinity Na^+/glucose cotransporter SGLT2, J. Clin. Invest. 93 (1994) 397–404.
[34] B.A. Hirayama, M.P. Lostao, M. Panayotoba-Heiermann, D.D.F. Loo, E. Turk, E.M. Wright, Kinetic and specificity differences between rat, human, and rabbit Na^+-glucose cotransporter (SGLT-1), Am. J. Physiol. 270 (1996) G919–G926.
[35] R. Novakova, D. Homerova, R.K.H. Kinne, E. Kinne-Saffran, J.T. Lin, Identification of a region critically involved in the interaction of phlorizin with the rabbit sodium-D-glucose cotransporter SGLT1, J. Membr. Biol. 184 (2001) 55–60.
[36] M.M. Raja, N.K. Tyagi, R.K.H. Kinne, Phlorizin recognition in a C-terminal fragment of SGLT1 studied by Trp scanning and affinity labeling, J. Biol. Chem. 278 (2003) 49154–49163.

[37] J.-T. Lin, J. Kormanec, D. Homerová, R.K.-H. Kinne, Probing transmembrane topology of the high-affinity sodium/glucose cotransporter (SGLT1) with histidine-tagged mutants, J. Membr. Biol. 170 (1999) 243–252.
[38] H. Jung, R. Rübenhagen, S. Tebbe, K. Leifker, N. Tholema, M. Quick, R. Schmid, Topology of the Na+/proline transporter of *Escherichia coli*, J. Biol. Chem. 273 (1998) 26400–26407.
[39] D.G. Gagnon, A. Holt, F. Bourgeois, B. Wallendorff, M.J. Coady, J.-Y. Lapointe, Membrane topology of loop 13–14 of the Na^+/glucose cotransporter (SGLT1): a SCAM and fluorescent labeling study, Biochim. Biophys. Acta 1712 (2005) 173–184.
[40] J.J. Mallee, T. Parella, H.M. Kwon, G.T. Berry, Multiple comparison of primary structure of the osmoregulatory Na+/myo-inositol cotransporter from bovine, human, and canine species, Mamm. Genome 7 (1996) 252.
[41] D.G. Gagnon, P. Bissonnette, J.-Y. Lapointe, Identification of a disulfide bridge linking the fourth and the seventh extracellular loops of the Na^+/glucose cotransporter, J. Gen. Physiol. 127 (2006) 145–158.